Spontaneous strain glass to martensite transition in a $Ti_{50}Ni_{44.5}Fe_{5.5}$ strain glass

Jian Zhang,[1,2,3,*] Yu Wang,[1,2] Xiangdong Ding,[1] Zhen Zhang,[1,2] Yumei Zhou,[1,2] Xiaobing Ren,[1,2,†] Dong Wang,[1] Yuanchao Ji,[1,2] Minghui Song,[2] Kazuhiro Otsuka,[1,2] and Jun Sun[1]

[1]*Multi-disciplinary Materials Research Center, Frontier Institute of Science and Technology, State Key Laboratory for Mechanical Behavior of Materials, Xi'an Jiaotong University, Xi'an 710049, China*

[2]*National Institute for Materials Science, 1-2-1 Sengen, Tsukuba 305-0047, Ibaraki, Japan*

[3]*Institute for Materials, Ruhr University Bochum, D-44801 Bochum, Germany*

(Received 16 June 2011; published 5 December 2011)

Glass transition has often been considered as a purely kinetics-controlled freezing process, thus it is not expected that a frozen glass state can spontaneously transform into a long-range-ordered (LRO) phase. Here we show evidence for a spontaneous transition from a frozen strain glass (STG) to a LRO martensite in a $Ti_{50}Ni_{44.5}Fe_{5.5}$ alloy: the alloy freezes into a STG at 179 K, but the frozen STG does not keep frozen and it transforms spontaneously into a LRO martensite (*R* phase) at 154 K. The transition from a frozen STG (with local *R*-like order) into a LRO *R* phase is explained by considering the existence of a thermodynamic driving force towards LRO. The present result indicates that thermodynamics may also play a role in glass, in addition to the kinetics.

DOI: 10.1103/PhysRevB.84.214201 PACS number(s): 64.70.P−, 64.60.Cn, 64.60.My

I. INTRODUCTION

Glass in a physics sense is a frozen state of certain "order,"[1,2] and has been found in a wide range of systems including amorphous (e.g., window glass), ferroic systems, polymers, and biological systems.[3,4] Despite its ubiquity in nature and extensive investigations, the origin of the glass transition is still one of the most intriguing open questions in materials science and condensed-matter physics.[4,5]

Many glasses can be formed by doping a sufficient amount of point defects or dopants into a system showing thermodynamic disorder-order transition.[6] The most familiar glass transition is the structural glass transition (i.e., amorphous), which can be viewed as the conjugate glass transition of liquid to crystal transition by doping a sufficient level of dopants. For example, doping gelatin into water can suppress the liquid-to-crystal transition and makes a liquid to glass (jelly)[6] Similarly, in ferroic systems, the conjugate glass transitions for ferroelectric and ferromagnetic transitions are the cluster dipolar glass (relaxor) and cluster spin-glass transition, respectively.[7,8] Recently, in another class of ferroic systems, the ferroelastic/martensitic systems, a conjugate glass has been discovered and named strain glass (STG) with sufficient doping of point defects, which suppresses the long-range-ordered (LRO) martensitic transformation[9–12] and was believed to remain frozen down to 0 K.[10] In sharp contrast with the conjugate disorder-order transitions that are due to the thermodynamic requirement of reducing entropy at low temperature, glass transitions are normally considered as due to a purely kinetic reason: frustration leads to drastic kinetic slowdown and eventually freezing.[13–15] As the consequence, it is not expected that an already kinetically "frozen" phase can further transform spontaneously into a LRO phase upon further cooling.

In this paper, we report that in a STG system ($Ti_{50}Ni_{44.5}Fe_{5.5}$) with local *R*-like strain order[16] there exists a spontaneous STG to martensite (a rhombohedral phase) transition from the already frozen STG state. Hereafter, spontaneous STG-*R* transition is used for short. This composition locates in the crossover composition regime from a normal martensite (lower than $Ti_{50}Ni_{45}Fe_5$) and STG (higher than $Ti_{50}Ni_{44}Fe_6$),[12] by including which we present a modified phase diagram of the $Ti_{50}Ni_{50-x}Fe_x$. We further show with the modified free-energy landscape of Ti-Ni-Fe STG, that the origin of this transition can be ascribed to the thermodynamic driving force towards a LRO phase, which drives the kinetically trapped system (i.e., the frozen STG state) into a more stable LRO phase. This mechanism may also explain similar spontaneous glass to LRO transition reported extensively in some ferroelectric relaxors.[17–20]

II. RESULTS

Figure 1 displays the temperature dependence of storage modulus and internal friction curves for $Ti_{50}Ni_{44.5}Fe_{5.5}$ at various frequencies (0.1, 0.2, 0.4, and 0.8 Hz) measured by DMA (dynamic mechanical analysis). Both the storage modulus and internal friction curves show frequency dispersion around $T_g \sim 182$ K, which follows the Vogel-Fulcher relation with $T_0 = 179$ K. This is characteristic of a STG transition, similar to that found in many other STG systems.[9,21] However, with further decreasing temperature 154 K (25 K below T_0), a new transition feature appears: the storage modulus curve show a frequency-independent kink: first softening and then hardening; the corresponding internal friction curve displays a peak, the position of which is independent of frequency, followed by a drop. It is in contrast to an ideal STG,[9,12,21] where the storage modulus increases continuously and the internal friction keeps decreasing with decreasing temperature for $T < T_0$, because of the gradual loss of mobility of the nanodomains due to further freezing of the system. Therefore the softening of storage modulus and corresponding internal friction peak at 154 K clearly indicate the existence of another transition from STG.

Now we show with *in situ* x-ray diffraction (XRD) and TEM that the anomaly is caused by a spontaneous STG-*R* transition, starting at $T_s = 154$ K as indicated with a red dotted line in Fig. 1. Note that the *in situ* XRD and TEM

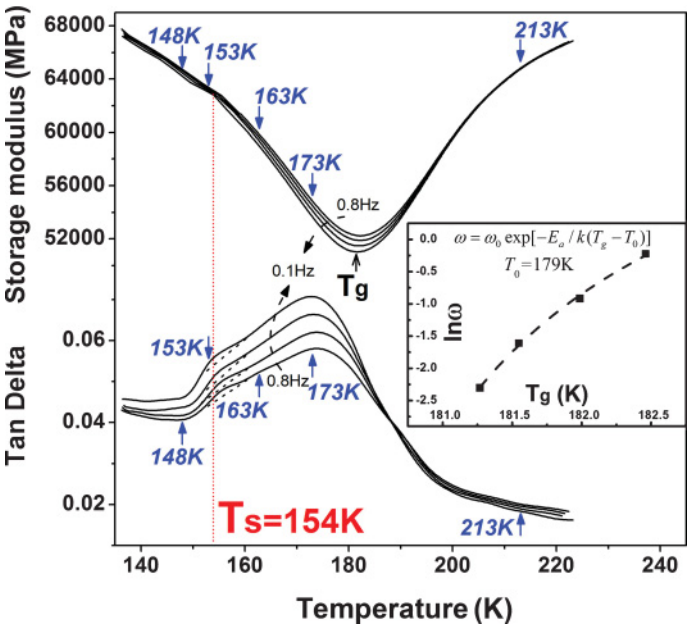

FIG. 1. (Color online) Temperature dependence of storage modulus and internal friction curves for $Ti_{50}Ni_{44.5}Fe_{5.5}$. T_0 (ideal frozen temperature) is obtained to be 179 K by fitting the frequency (ω) dependence of $T_g(\omega)$ (STG transition temperature) with the Vogel-Fulcher relation $\omega = \omega_0 \exp[-E_a/k(T_g - T_0)]$, in the inset. Around 154 K (T_s), internal friction shows broad humps and storage modulus displays kinks. The five pairs of blue arrows indicate five temperatures of TEM observations in Fig. 4.

data presented below have a strong similarity to those of the spontaneous transition from relaxor to LRO ferroelectrics in relaxor.[20] In Fig. 2, the 110_{B2} XRD peak of $Ti_{50}Ni_{44.5}Fe_{5.5}$ keeps a singlet with slight broadening from 213 to 163 K spanning the STG transition temperature, $T_0 = 179$ K; this is expected for a STG transition that is not associated with a change in the average cubic ($B2$) structure.[10] When the temperature is further lowered to 153 K, which is below the DMA anomaly temperature in Fig. 1, the peak further broadens and shows apparent asymmetry in shape. It suggests that the 110_{B2} peak starts to split, although the peak still remains as a singlet. Lorentzian peak fitting indicates that two additional peaks appear, which can be indexed as 112_R and 300_R R-phase peaks, respectively, although the new peaks are still low in intensity. Therefore no obvious splitting is probably due to the very small R-distortion and volume fraction of formed R phase at the temperature close to the T_s, which cannot be differentiated by the conventional XRD used in the present study. Moreover, the intensity and splitting of these two R peaks increase with the decrease of temperature gradually. It can be understood as the gradual growth R phase both in size and in volume fraction during cooling. The above results provide direct evidence for the spontaneous STG-R transition. For clarity, the lattice parameters (d spacings) of 110_{B2}, 112_R, and 300_R peaks are plotted versus temperature in Fig. 3. It shows the lattice parameter of 110_{B2} decrease linearly with the decrease of temperature down to 154 K, which spans the STG transition with $T_0 = 179$ K; the lattice parameter changes discontinuously around $T_s = 154$ K, from STG to R phase.

In situ TEM results (Fig. 4) reveal microscopically how the system evolves during both the STG and spontaneous STG-R transition. Emphasis is put on what happens in the three characteristic temperature ranges shown in Fig. 3: (1) $T > T_0$, unfrozen STG; (2) $T_0 > T > T_s$, frozen STG; (3) $T < T_s$, R phase.

Figure 4(a) shows a bright-field image of the sample at 213 K ($T > T_0$), where the system is in an unfrozen STG state. Only sparse and faint nanodomains are visible with a size around 8 nm. The faintness of nanodomains can be ascribed to the small distortion with respect to the $B2$ lattice. It coincides with weak diffuse scattering along three $\langle 110 \rangle_{B2}$ directions in the corresponding diffraction pattern [see inset in Fig. 4(a)]. When the temperature decreases to 173 K($T_0 > T > T_s$), where the DMA results (Fig. 1) indicate a frozen STG state, the image in Fig. 4(b) shows full occupation of randomly distributed nanodomains, the size of which coarsens up to around 11 nm. Correspondingly, its diffraction pattern [inset of Fig. 4(b)] shows stronger diffuse scattering. Upon further cooling to 163 K($T_0 \gg T > T_s$), the size of nanodomains (~12 nm) does not increase much, as shown in Fig. 4(c) whereas the contrast of nanodomains becomes higher, which corresponds to a little condensation of diffuse scattering intensity located closer to commensurate $1/3\langle 110 \rangle_{B2}$ positions in the diffraction pattern shown in the inset of Fig. 4(c).

In contrast with the conventional expectation that the already frozen glass should not undergo any further change upon further cooling, the frozen STG in $Ti_{50}Ni_{44.5}Fe_{5.5}$ undergoes an interesting change at 153 K ($T \sim T_s$), as shown in Fig. 4(d). Although the overall random feature of the nanodomain morphology does not change, the size of the nanodomains grows and some can reach 50 nm [e.g., the right corner of Fig. 4(d)]. At such a size the nanodomains can be detected by XRD as R phase and hence account for the new R peaks of small splitting and very low intensity at the 153 K XRD line (Fig. 2). It indicates that the microscopic morphology has not yet changed much although the system becomes active (the softening of storage modulus leads to the greater mobility of the nanodomain and hence an internal friction peak) according to the DMA results (Fig. 1).

With further cooling to 148 K, some nanodomains are aligned to form platelike R variants with the dimension around 100×20 nm^2 and the rest still remains in random nanodomains (i.e., frozen STG) as displayed in Fig. 4(e). At 123 K ($T \ll T_s$), the image [Fig. 4(f)] shows the growth of R "plate" as well as the remaining nanodomains. When

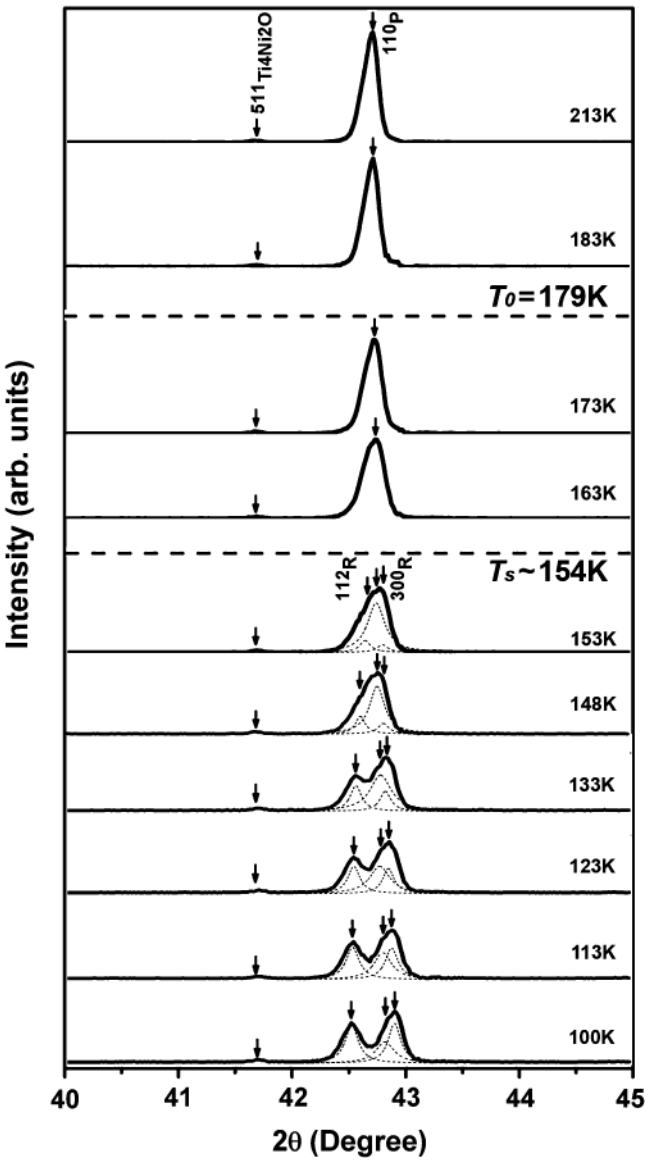

FIG. 2. XRD lines for $Ti_{50}Ni_{44.5}Fe_{5.5}$ STG at constant temperatures on cooling. The dashed peaks underneath the experimental peak profiles (below the T_s) are Lorentzian peaks, which give the best fit to the experimental profiles.

the temperature reaches 100 K [Fig. 4(g)], the image shows that the R "plate" grows not only in size (150×30 nm^2) but also in density. Note that even at 100 K, there still exist a small portion of nanodomains [upper right corner of Fig. 4(g)], which explains the remnant weak 110_{B2} XRD peak at 100 K in Fig. 2. The above results also show that the spontaneous STG-R transition progresses rather gradually from frozen STG (randomly distributed R-like nanodomains) to LRO R phase through a gradual alignment of local R-like nanodomains in $Ti_{50}Ni_{44.5}Fe_{5.5}$ and a small portion of frozen R-like nanodomains still remains even down to 100 K, which is consistent with the XRD results in Fig. 2. Note that the "island-chain" morphology of the R "plate" is somewhat different from that of a typical "herringbone" normal R phase.[22] Our finding experimentally proves the prediction of a mixed STG and martensite state by a pseudospin Landau-Ginzburg modeling

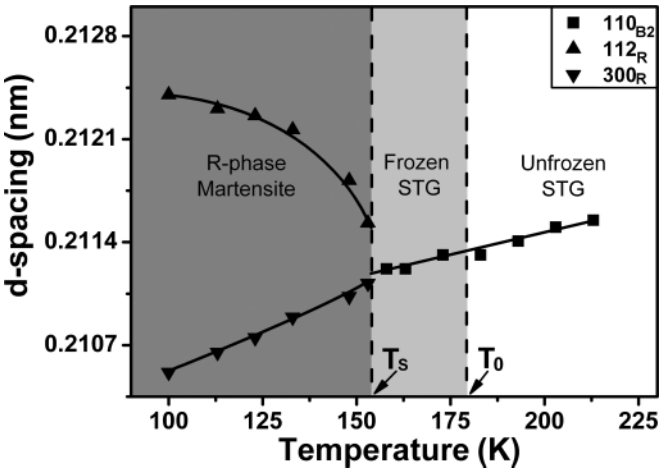

FIG. 3. Temperature dependence of d-spacings of 110_{B2}, 112_R, and 300_R peaks from XRD lines shown in Fig. 2 during cooling. T_s defined in Fig. 1 coincides with the starting temperature of the splitting of 110_{B2} peak into 112_R and 300_R peaks.

of martensitic alloys,[23] utilizing mathematical mapping to a spin glass.

According to the qualitative predicted phase diagram in Ref. 23, a modification has been made to the previous $Ti_{50}Ni_{50-x}Fe_x$ phase diagram,[16] where a crossover composition regime ($5 < x_{cr}^{left} \leqslant x \leqslant x_{cr}^{right} < 6$) is added based on the finding of spontaneous STG-R transition in $Ti_{50}Ni_{44.5}Fe_{5.5}$ as shown in Fig. 5. Besides, the critical composition x_c for the STG formation is modified to be equal to the left composition limit of the crossover regime, which is slightly larger than 5, i.e., $x_c = x_{cr}^{left}$. Note that a similar phase diagram, including a crossover composition regime undergoing spontaneous relaxor to ferroelectric phase transition, can be found in parallel relaxor ferroelectric systems.[24,25]

To avoid confusion, it is worth mentioning that all phases in Fig. 5 are crystalline/LRO states with respect to the order parameter of atomic configuration, based on which the crystallization and vitrification processes can be designated to disorder → order and disorder → frozen disorder transition.[26] While the disorder/order labeled in the square under each phase refers to long-range disorder/order of the order-parameter strain, which describes the ferroelastic/martensitic transformation as disorder → order transition and the STG transition as disorder → frozen disorder transition. Moreover, the long-range strain disordered states (with $B2$ crystallographic structure) all possess R-like local strain order, no matter whether it is dynamic (parent phase with no static nanodomain), quasidynamic (precursor and unfrozen STG with less sticky or sticky nanodomains), or frozen disorder (STG with frozen nanodomains). Here the stickiness refers to the slow mechanic response of nanodomains, which can be detected by DMA and manifested with a slight frequency dispersion before STG transition.[6] Note that the DMA test is a critical technique to differentiate the STG from the precursor, since STG transition is a kinetic freezing down process and manifested with frequency-dependent storage modulus dips and internal friction peaks, although they may look similar in the static microscopic morphology captured by TEM images.

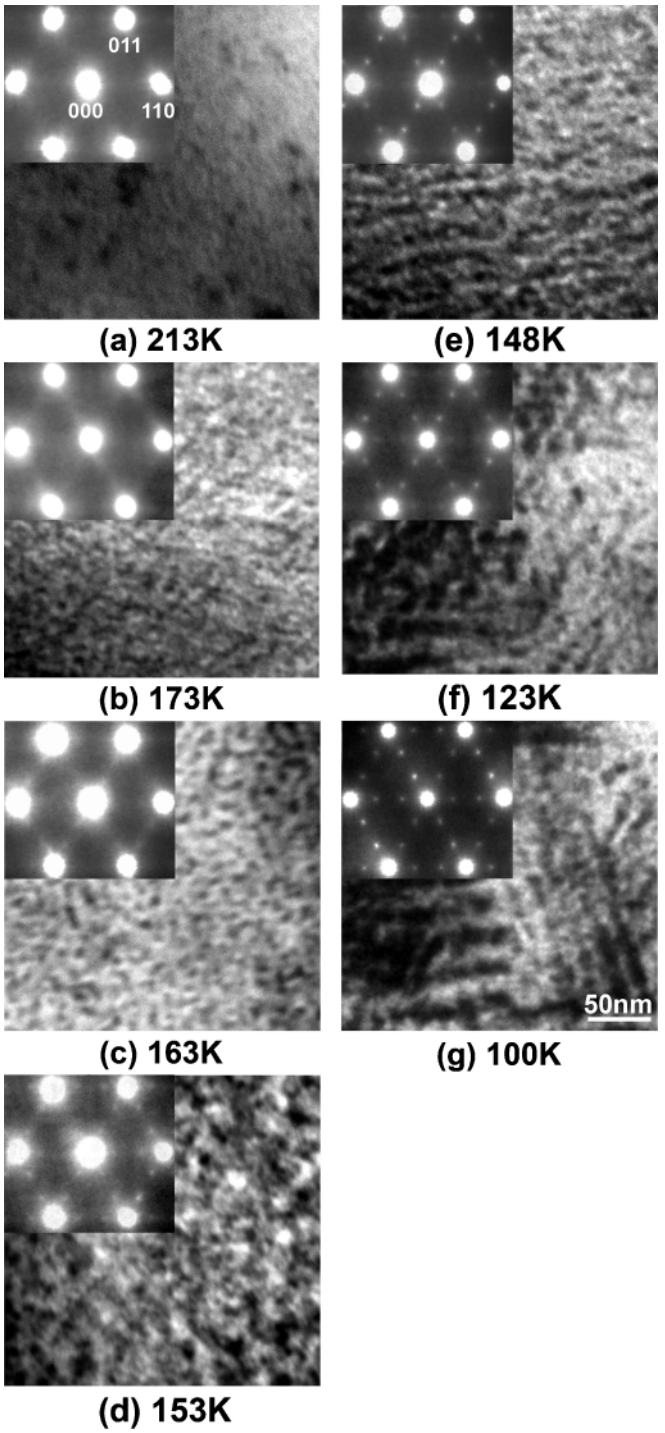

FIG. 4. Bright-field images of $Ti_{50}Ni_{44.5}Fe_{5.5}$ observed at three temperature regimes indicated in Fig. 3: $T > T_0$ (213 K), $T_s < T < T_0$ (173 and 163 K) and $T < T_s$ (153, 148, 123, and 100 K), respectively, and the insets are the corresponding diffraction patterns with $[1\bar{1}1]$ zone axis.

The further discussion of the modified phase diagram will be presented later on the basis of the understanding of spontaneous STG-*R* transition presented below.

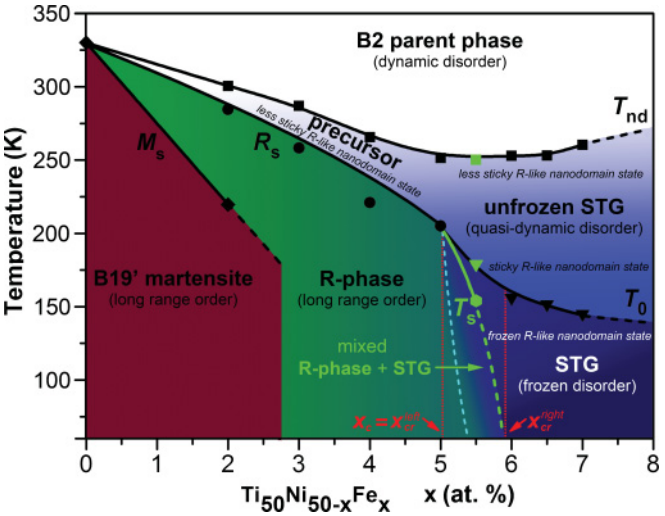

FIG. 5. (Color online) Modified phase diagram of $Ti_{50}Ni_{50-x}Fe_x$ system (Ref. 16) with the addition of a crossover composition regime ($5 < x_{cr}^{left} \leqslant x \leqslant x_{cr}^{right} < 6$), where it undergoes STG transition followed by spontaneous STG-*R* transition during cooling. x_{cr}^{left} and x_{cr}^{right} denote the left and right border compositions of crossover regime. x_{cr}^{left} is defined as the critical composition of STG formation, namely $x_c = x_{cr}^{left}$. T_{nd}(■) is the starting temperature of the appearance of precursory nanodomain; R_s(●) and M_s(◆) are the martensitic transformation starting temperatures for *R* phase and *B*19′ martensites, respectively; T_0(▼) is the STG transition temperature (i.e., ideal frozen temperature); T_s(●) is spontaneous STG-*R* transition starting temperature. The symbols for $Ti_{50}Ni_{44.5}Fe_{5.5}$ characteristic temperatures are highlighted in green (gray) color, such as T_{nd}(■), T_0(▼), and T_s(●). The dotted lines are a guide to the eye.

III. DISCUSSION

The above experimental facts provide clear evidence for the spontaneous transition from a frozen STG to a long-range strain order. This is a very interesting result since it means that a "dormant" or frozen STG can be "awakened" at low temperature. This is unexpected considering the STG is formed solely due to a kinetic reason. It suggests that the thermodynamic factor or driving force may also play a role in STG and other glassy transitions, as described further below. (1) Thermodynamic driving force, which is inherited from thermodynamic counterpart and favored LRO phase, triggers the local ordering (nanodomains/nuclei of LRO phase) and hence determines the local order of glass; while the drastic slowing down of kinetics is caused by local energy barriers, which are due to the random field of the point defects. (2) Both the thermodynamic driving force and local barriers evolve during cooling; the glass state may appear if the LRO phase cannot be reached above the kinetic frozen temperature (i.e., T_0 in STG), where an anomaly of dynamic susceptibility appears (storage modulus in STG). (3) Upon further cooling, the thermodynamic driving force may overcome the local barriers at a certain temperature (such as T_s in STG), which promotes the further growth of nanodomains and finally the system may start to transform to LRO phase. Hence it becomes comprehensible why the spontaneous STG-*R* transition only occurs within the crossover composition regime, since the local barriers in such a regime are not significantly high and

hence the system may partially or totally transform before the thermal activation energy gets too low as temperature approaches 0 K. It also explains why the nanodomains in both Ti-Ni and Ti-Ni-Fe STGs possess *R*-like local strain order as they both possess LRO *R*-phase instability.[16]

A. Phenomenological explanation of the spontaneous STG-*R* transition in Ti-Ni-Fe ternary STG

In the following we present a modified phenomenological explanation for the STG transition [Figs. 6(a)–6(c)] and the subsequent spontaneous STG-*R* transition [Figs. 6(d)–6(f)] in $Ti_{50}Ni_{44.5}Fe_{5.5}$. We utilize the free-energy landscape recently proposed for STG,[16,27] but add a new factor: the thermodynamic driving force ($\Delta G_{B2\to R}$) toward long-range order (*R* phase).

In Figs. 6(a)–6(c), $\Delta G_{B2\to R} < 0$, the system stays in the STG valley with zero average strain. For the free-energy landscape of $T_s < T < T^*$ shown in Fig. 6(d), $\Delta G_{B2\to R}$ becomes positive, but the system is still in the frozen STG state since the thermodynamic driving force $\Delta G_{B2\to R}$ is still smaller than $E_{LB} - k_BT$, which means the thermodynamic driving force cannot draw the system from the stuck position in phase space into the LRO *R* phase with the help of thermal activation energy.

When the temperature further decreases to T_s [in Fig. 6(e)], where $\Delta G_{B2\to R}$ becomes comparable to $E_{LB} - k_BT$, the spontaneous STG-*R* transition occurs. As the temperature further lowering $T < T_s$, it is expected that the system transforms into *R* phase completely within limited temperature range. However, from the XRD and TEM results shown in Figs. 2 and 4, respectively, the spontaneous STG-*R* transition does not complete even down to 100 K, where a small portion of frozen STG (random nanodomains) still remains. It can be understood as follows: since the system is highly defected with Fe, the growth of the LRO *R* "plate" (with uniform strain direction) will build up one internal stress field opposing the strain direction of the LRO *R* (caused by the random stress field of point defects against the long-range ordering), which will tilt the free-energy landscape and hence lower the $\Delta G_{B2\to R}$ and finally lead to the stopping of the *R* "plate" growth. This stress field is also against the LRO of nanodomains around the plate. Thus it can explain the irregular shape of the *R* plate as well as the remnant of nanodomains.

B. A modified phase diagram of $Ti_{50}Ni_{50-x}Fe_x$ ferroelastic system

The discussion above reveals the important role of thermodynamic driving force on the spontaneous transition from frozen STG to the *R* phase. It also indicates that the doping of Fe (increasing point defect concentration) not only affects the thermodynamic properties of the system (decreasing R_s and M_s by destabilizing the *R* phase, $B19'$ martensites),[12] but also the kinetic properties of the system (the slowing down of transition kinetics, due to the increase of E_{LB} caused by increasing random local stress field of point defects). Subsequently, a brief discussion on the modified phase diagram of $Ti_{50}Ni_{50-x}Fe_x$ system (Fig. 5) is proposed by carefully describing four representative composition/composition regimes as follows:

(1) $x = 0$, i.e., $Ti_{50}Ni_{50}$ ($B2 \to B19'$).

No static *R*-like nanodomain can be observed prior to the martensitic transformation ($B19'$), since Ti-Ni is a strongly (crystallographic) ordered alloy and ideally has no point defects,[28] i.e., $E_{LB} \sim 0$. The system transforms directly from the parent phase with dynamic disorder (local cooperative *R*-like distortion of lattice) into $B19'$ martensite.

(2) $0 < x < x_c(=x_{cr}^{left})$, normal *R*-phase transformation.

At $T > T^*$, $E_{LB} < k_BT$: the static *R*-like nanodomains start to appear at T_{nd}; the stickiness of the nanodomain increases with the increase of x due to the increase of E_{LB}; when $x \to x_c$, the nanodomain state is going to be, but not yet, frozen into STG at R_s, where E_{LB} is still slightly smaller than k_BT. Note that the nanodomain state in this region was termed premartensitic tweed or precursor, which is not differentiable from the unfrozen STG state ($x \geqslant x_c$) at relative high temperature with high defect concentration in both static (microscopic morphology) and dynamic (less stickiness) aspects.[6] In contrast, the precursory nanodomain state transforms into the LRO *R* phase upon further cooling, while the latter becomes more sticky (showing slight frequency dispersion in the vicinity of T_0) and freezes into STG before the system reaches thermodynamic equilibrium temperature T^*.

At $T = R_s < T^*$, $\Delta G_{B2\to R} > E_{LB} - k_BT$: the system transforms into the *R* phase instead of freezing into the STG state. Besides, the kinetics of *R*-phase transformation also slows down with the increase of x due to the increase of E_{LB}, which might be the reason for the greater decrease of R_s during $x \to x_c$.

(3) $x_c \leqslant x \leqslant x_{cr}^{right}$, crossover region.

At $T > T_0 \gg T^*$, $E_{LB} < k_BT$: upon cooling from high temperature, the system changes gradually from a dynamic disordered parent phase to a less sticky nanodomain state at T_{nd}, and to a sticky nanodomain state with $T \to T_0$ while E_{LB} increases and approaches k_BT.

At $T^* < T \leqslant T_0$, $E_{LB} \geqslant k_BT$: the system freezes into the frozen STG state at T_0 [Fig. 6(b)], and becomes more frozen due to the increase of $E_{LB} - k_BT$ during cooling, which corresponds to decreasing mobility of nanodomains.

At $T_s < T \leqslant T^*$, $\Delta G_{B2\to R} < E_{LB} - k_BT$: the system is awakening from the deep frozen state with $\Delta G_{B2\to R} - (E_{LB} - k_BT)$ increasing and approaching zero upon cooling [Figs. 6(c) and 6(d)].

At $T \leqslant T_s$, $\Delta G_{B2\to R} \geqslant E_{LB} - k_BT$: when the temperature reaches T_s, the system starts to transform into the LRO *R* phase [Fig. 6(e)], which may proceed completely into a normal *R* phase at $x_c \leqslant x < 5.5$ or stop in a mixture of *R* phase and STG state $5.5 \leqslant x \leqslant x_{cr}^{right}$ since the E_{LB} is relatively small for the former and relatively large for the latter.

(4) $x > x_{cr}^{right}$, STG region (STG remains frozen until 0 K):

The phenomena that occur in this region during cooling are essentially similar to those in the crossover regime as described above. The only difference is that the STG state remains frozen until 0 K without further transforming to *R* phase (i.e., no spontaneous STG-*R* transition), since the thermodynamic stability of the *R* phase decreases and the E_{LB} increases with further doping of Fe (at $T \leqslant T^* \ll T_0$, $\Delta G_{B2\to R} < E_{LB} - k_BT$).

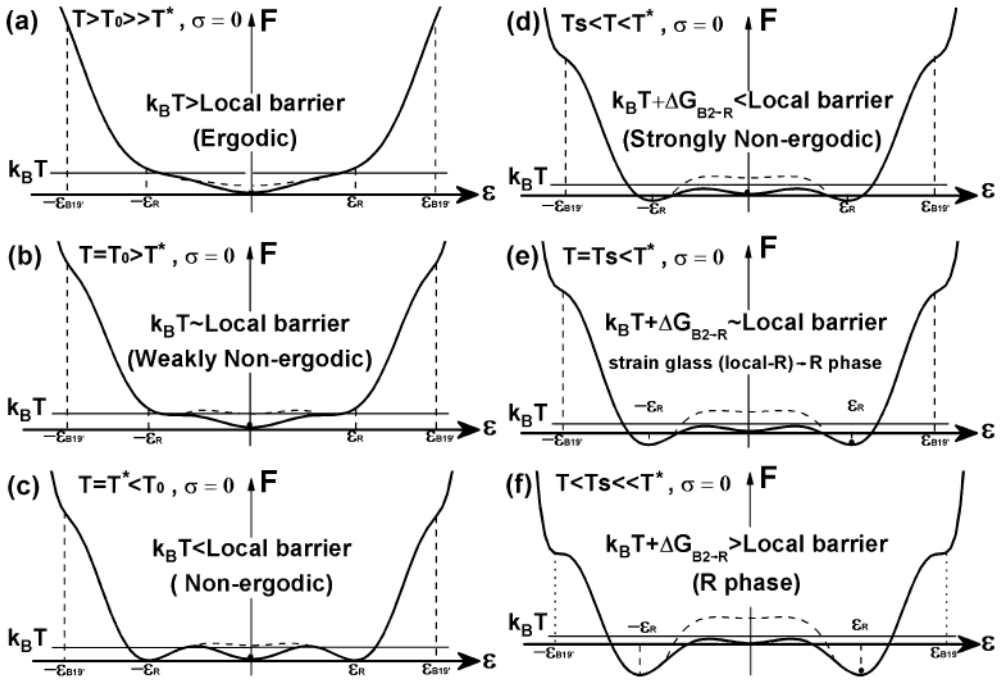

FIG. 6. Phenomenological explanation for the free-energy evolution during the STG transition and the subsequent spontaneous STG-*R* transition in $Ti_{50}Ni_{44.5}Fe_{5.5}$. T^* is the temperature where *R* phase starts to be stable; F is the free energy; k_BT is the thermal activation energy; and $\Delta G_{B2\rightarrow R}$ is the thermodynamic driving force for *B*2 transforming into *R* phase; ε_R and $\varepsilon_{B19'}$ are the strains for the potential *R* and $B19'$ martensites, respectively. The curved solid line is for the average strain (ε) dependence of the average free energy (F) of all the microscopic configurations corresponding to a given macroscopic strain state, and the dashed line represents the average local free-energy barriers (E_{LB}).

From the discussion above, one can see that the crossover from normal martensitic transformation to STG transition is continuous over a composition region rather than abrupt at one composition, which suggests the underlying relationship between them as follows. Martensitic phase transition is a thermodynamically driven process that may be slowed down by the random local stress field (E_{LB}) of point defects ($x < x_c$). With doping a sufficient amount of point defect ($x \geqslant x_c$), the E_{LB} may become larger than thermal activation energy k_BT before the system reaches thermodynamic equilibrium temperature T^*, hence the martensitic transformation is suppressed and the system freezes into the STG state. The frozen STG state may remain dormant and no martensite will appear, if $\Delta G_{B2\rightarrow R} < E_{LB} - k_BT$ is valid down to 0 K. However, the frozen STG is not always dormant and may be awakened to transform into LRO martensite when E_{LB} is not so large in the crossover composition range. In another word, STG transition is a kinetic dominant process, by masking the thermodynamic driving force, which can be enhanced and regains the power through exerting stress field (stress induced STG to martensite transition)[10,16] or further cooling (spontaneous STG-*R* transition). Furthermore, it will be interesting to see the STG transition in the AuCd system where the random local stress field may be finely tuned by manipulating highly mobile point defects,[29,30] through which the relationship between thermodynamic driving force and kinetic local barrier may be modified and even altered.

IV. CONCLUSIONS

In conclusion, we report that $Ti_{50}Ni_{44.5}Fe_{5.5}$ STG ($T_0 =$ 179 K) undergoes a spontaneous transition from STG (local *R*-like strain order) into the *R* phase at $T_s = 154$ K, based on which a modified phase diagram of the Ti-Ni-Fe ferroelastic system is presented. Furthermore, we provide a phenomenological model to show that the origin of the spontaneous STG-*R* transition is due to thermodynamic driving force to the underlying LRO phase. It also suggests that the STG transition is not solely due to kinetic reasons; instead it is a result of competition between thermodynamic driving force to LRO and kinetic frustration caused by local barriers that favor a frozen disordered state: the system is trapped in glassy state when the thermodynamic LRO transition is suppressed by local barriers; thermodynamic driving force can regain the power once it becomes stronger than kinetics by temperature as well as stress-field variations, i.e., spontaneous and field-induced glass to LRO transitions, otherwise, the system remains in the frozen glassy state. Our explanation evokes the link of the STG transition to the underlying LRO ferroic transitions, and thus should be applicable to other ferroic cluster glasses. Moreover, it may be a comment on other kinds of glasses: glass transition is a thermodynamically (LRO and entropy lowering) driven but kinetics-controlled process, for all the glass transitions should bear the same physical nature. It may also settle the dispute on whether the glass transition is a purely kinetic process.

ACKNOWLEDGMENTS

This work was supported by Kakenhi of JSPS, National Natural Science Foundation of China (Grants No. 51171140 and No. 51101118), National Basic Research Program of China (Grants No. 2010CB631003 and No. 2012CB619401), and 111 project of China (Grant No. B06025). J.Z. acknowledges funding by SFB 459 at RUB, and by Alexander von Humboldt Foundation.

*zhang.jian@rub.de

†Ren.Xiaobing@nims.go.jp

[1] J. A. Mydosh, *Spin Glasses* (Taylor & Francis, Philadelphia, 1993).

[2] K. Binder, *Glassy Materials and Disordered Solids* (World Scientific, London, 2005).

[3] C. A. Angell, Science **267**, 1924 (1995).

[4] A. P. Sokolov, Science **273**, 1675 (1996).

[5] S. Torquato, Nature (London) **405**, 521 (2000).

[6] X. B. Ren *et al.*, Philos. Mag. **90**, 141 (2010).

[7] R. T. Zhang, J. F. Li, and D. Viehland, J. Am. Ceram. Soc. **87**, 864 (2004).

[8] R. N. Bhowmik and R. Ranganathan, J. Magn. Magn. Mater. **248**, 101 (2002).

[9] S. Sarkar, X. Ren, and K. Otsuka, Phys. Rev. Lett. **95**, 205702 (2005).

[10] Y. Wang, X. B. Ren, and K. Otsuka, Phys. Rev. Lett. **97**, 225703 (2006).

[11] Y. Wang, X. Ren, K. Otsuka, and A. Saxena, Phys. Rev. B **76**, 132201 (2007).

[12] D. Wang, Z. Zhang, J. Zhang, Y. Zhou, Y. Wang, X. Ding, Y. Wang, and X. Ren, Acta Mater. **58**, 6206 (2010).

[13] W. Gotze and L. Sjogren, Rep. Prog. Phys. **55**, 241 (1992).

[14] L. Santen and W. Krauth, Nature (London) **405**, 550 (2000).

[15] B. Jerome and J. Commandeur, Nature (London) **386**, 589 (1997).

[16] J. Zhang, Y. Wang, X. Ding, Z. Zhang, Y. Zhou, X. Ren, K. Otsuka, J. Sun, and M. Song, Phys. Rev. B **83**, 174204 (2011).

[17] X. H. Dai, Z. Xu, and D. Viehland, J. Am. Ceram. Soc. **79**, 1957 (1996).

[18] P. G. Debenedetti and F. H. Stillinger, Nature (London) **410**, 259 (2001).

[19] A. A. Bokov and Z. G. Ye, J. Mater. Sci. **41**, 31 (2006).

[20] X. H. Dai, Z. Xu, and D. Viehland, Philos. Mag. B **70**, 33 (1994).

[21] Y. M. Zhou *et al.*, Acta Mater. **58**, 5433 (2010).

[22] K. Otsuka and X. Ren, Prog. Mater. Sci. **50**, 511 (2005).

[23] D. Sherrington, e-print arXiv:1007.1530 (to be published).

[24] J. Ravez, C. Broustera, and A. Simon, J. Mater. Chem. **9**, 1609 (1999).

[25] H. C. Liu, R. Harrison, and A. Putnis, J. Appl. Phys. **90**, 6321 (2001).

[26] G. Careri, *Order and Disorder in Matter* (Benjamin/Cummings, San Francisco, 1984).

[27] Y. Wang, X. Ren, K. Otsuka, and A. Saxena, Acta Mater. **56**, 2885 (2008).

[28] J. Zhang *et al.*, Acta Mater. **55**, 2897 (2007).

[29] X. B. Ren and K. Otsuka, Nature (London) **389**, 579 (1997).

[30] J. Deng, X. Ding, T. Lookman, T. Suzuki, A. Saxena, K. Otsuka, J. Sun, and X. Ren, Phys. Rev. B **82**, 184101 (2010).